Optics Letters

Achieving comb formation over the entire lasing range of quantum cascade lasers

YANG YANG,[1,*] DAVID BURGHOFF,[1] JOHN RENO,[2] AND QING HU[1]

[1]Department of Electrical Engineering and Computer Science, Research Laboratory of Electronics, Massachusetts Institute of Technology, Cambridge, Massachusetts 02139, USA
[2]Center for Integrated Nanotechnology, Sandia National Laboratories, Albuquerque, New Mexico 87123, USA
*Corresponding author: yang_y@mit.edu

Received 31 May 2017; revised 23 August 2017; accepted 6 September 2017; posted 7 September 2017 (Doc. ID 297094); published 25 September 2017

Frequency combs based on quantum cascade lasers (QCLs) are finding promising applications in high-speed broadband spectroscopy in the terahertz regime, where many molecules have their "fingerprints." To form stable combs in QCLs, an effective control of group velocity dispersion plays a critical role. The dispersion of the QCL cavity has two main parts: a static part from the material and a dynamic part from the intersubband transitions. Unlike the gain, which is clamped to a fixed value above the lasing threshold, dispersion associated with the intersubband transitions changes with bias, even above the threshold, and this reduces the dynamic range of comb formation. Here, by incorporating tunability into the dispersion compensator, we demonstrate a QCL device exhibiting comb operation from I_{th} to I_{max}, which greatly expands the operation range of the frequency combs.

OCIS codes: (140.5965) Semiconductor lasers, quantum cascade; (230.2035) Dispersion compensation devices.

https://doi.org/10.1364/OL.42.003888

Frequency combs are broadband coherent light sources that consist of large numbers of evenly spaced lasing modes. It has been demonstrated that broadband QCLs can form frequency combs [1,2]. In the terahertz regime, QCL-based frequency combs offer compactness and high output power, showing great promise for broadband spectroscopy. QCL combs can be combined with traditional Fourier spectroscopy as bright broadband sources [3], or can be constructed into a dual-comb configuration for high-speed spectroscopy [4]. To achieve comb operation in QCLs with the phase-locking arising from four-wave mixing [5], one needs to manage the group velocity dispersion (GVD). Two major contributions are important to the dispersion in QCLs. The first one, waveguide dispersion and dispersion from the "Reststrahlen band" of the host semiconductor, provides a static contribution to the dispersion, which is unaffected by the laser bias. In contrast, intersubband transitions give rise to a bias-dependent dispersion. Unlike gain that is clamped to the total loss above the lasing threshold, the dispersion changes, even above the threshold, as a consequence of the change in the lineshape of the gain curve [6].

In order to make terahertz QCLs operate as combs, two different approaches have been pursued to engineer the cavity dispersion. One is to design a dispersion compensator (DC) with negative GVD to cancel the positive cavity dispersion so that the overall dispersion in the frequency range of interest is low [2]. Gain medium engineering is another option. By combining several different gain media, the resulting heterogeneous gain medium has a relatively flat gain top, within which the intrinsic dispersion is small enough to preserve comb formation [7]. Although interesting results have been demonstrated using both methods, both of them are ineffective in handling the bias-dependent dispersion. In the case of the DC, the careful design can only be applied to a narrow bias range. In addition, in the case of gain medium engineering, the flat top gain is also only implemented at the desired bias point and, moreover, the heterogeneous nature of that gain media entangles the dispersion dynamics at other biases. As a result, the comb mode operation in the best device with a DC covers about 29% of the entire lasing bias range [2], while the corresponding number from the best gain-medium-engineered device is about 23% [7].

To address the bias-dependent dispersion issue, we have designed and implemented a dispersion-compensated QCL in a two-section configuration. The device consists of a Fabry–Perot (FP) section and a DC section with a 2 μm gap. This narrow gap allows the DC section to be independently biased which effectively balances the bias-dependent dispersion of the FP section. From the threshold current to its maximum current—I_{th} to I_{max}—the device can operate as a frequency comb with the broadest spectrum coverage of about 600 GHz at 3.5 THz, making it a valuable tool for QCL comb-based spectroscopy.

In order to compensate for the dispersion, the cavity dispersion has first been characterized using terahertz time domain spectroscopy in the self-referenced geometry. Detailed information about the characterization techniques and measured dispersion relating to this work is well documented in Ref. [6]. A nonlinear phase-frequency relation is associated with the dispersion. For example, the measured phase (average group delay removed) from a 5 mm long FP cavity is plotted with light blue in Fig. 1(c). With this knowledge, a DC is designed

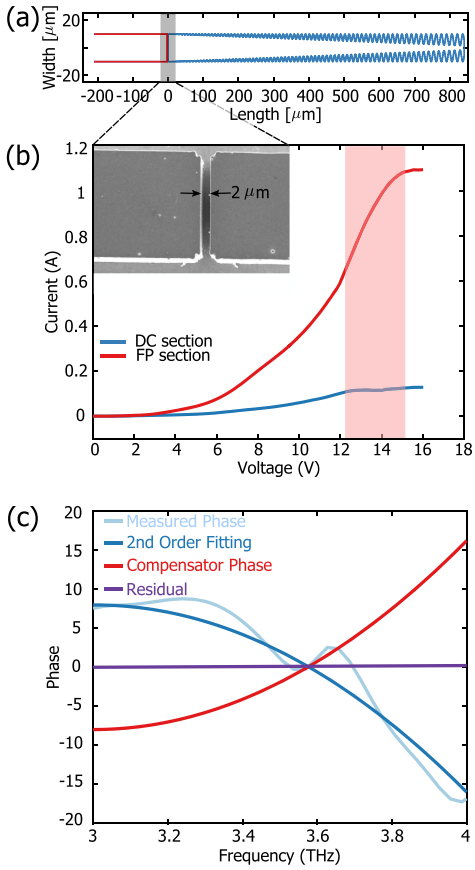

Fig. 1. (a) Schematic of the device in a two-section configuration. The DC section is shown in blue; part of the FP section is in red. (b) Current-voltage characteristics for each section. The pink-shaded area indicates the entire dynamic range of lasing, from I_{th} to I_{max}. The inset shows the SEM photo for the air gap in the real device. (c) The nonlinear part of the measured phase from a 5 mm long FP cavity is shown in light blue. The second-order fitting for that phase is shown in blue. The calculated phase from the DC is shown in red, while the phase residual is shown in purple.

to cancel the nonlinear phase within the frequency range of interest. In general, any sidewall corrugation that introduces refractive index change can serve as a DC. Here, we choose to use the well-established double-chirped sinusoidal structure [2,8,9] with optimized parameters based on the measured phase data. To compensate for the dispersion, the period of the sinusoidal corrugation is linearly chirped from 8.5 to 15.75 μm, and the corrugation's amplitude is chirped in the same way to avoid any oscillation in the group delay due to Gires-Tournois-like interference. As a result, a 841 μm long DC section possesses a 2nd-order dispersion of −1.3919 ps^2 in the range of 3–4 THz. Shown in red and blue, respectively, are the phase calculated from the optimized DC section, as well as the second-order fitting of the measured phase. The residual after matching phases, shown in purple in Fig. 1(c), is negligible.

The schematic for the real device is illustrated in Fig. 1(a). A 2 μm wide air gap is defined and etched between the FP section and the DC section. The insert in Fig. 1(b) shows the scanning electron microscope (SEM) of the defined air gap in the actual device. This narrow gap allows these two sections to be electrically isolated while remaining optically coupled [10].

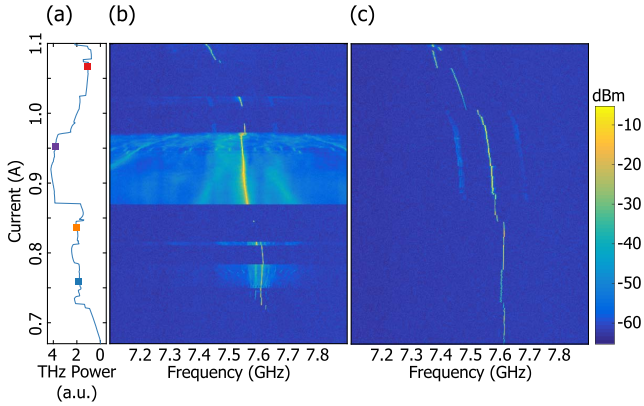

Fig. 2. (a) Output light characterization over the laser's dynamic range of lasing. (b) Repetition-rate beatnote map in the corresponding bias range with the DC section unbiased. (c) Repetition-rate beatnote map in the same bias range with the DC section biased to the optimal point for each FP section bias.

Figure 1(b) shows the current-voltage characteristics for each section at 25 K. The pink-shaded area indicates the entire dynamic range of lasing, I_{th} to I_{max}, within which the output light characterization is shown in Fig. 2(a).

One key indication of comb formation in QCLs is a strong beatnote at the laser's repetition rate, $f_{rep} = c/2nL$. A narrow and strong repetition beatnote implies that the dispersion inside the laser cavity is sufficiently low so that the four-wave mixing process can lock the lasing modes to be evenly spaced with a mode spacing of f_{rep}, i.e., the device is under the comb operation. Other situations do exist. Lacking or insufficient dispersion compensation can result in broad beatnotes, or multiple beatnotes, both of which indicate the lasing modes inside the cavity lack coherence [11], and the device is behaving like a regular multi-mode laser. To gain insights about the comb performance over the entire dynamic range, repetition-rate beatnote signals are recorded from I_{th} to I_{max} from a bias tee, which is attached to the bias line of the FP section.

The repetition-rate map from the device with the DC section unbiased is shown in Fig. 2(b). It is clear that within the entire dynamic range of lasing, the repetition-rate beatnote exhibits different states, as described before. In addition, comb formation featuring a narrow repetition-rate beatnote only exists within a limited biasing range and is interspersed with broad beatnote, multi-beatnote, and no beatnote regimes. The complex beatnote dynamics shown in Fig. 2(b) is not a unique case, and it happens in almost all previously reported terahertz QCL comb publications [2,7,11,12].

Differing from all of the previous works, in Fig. 2(c) we show the beatnote map within the same bias range, but with the DC section's bias optimized for a strong single beatnote at each bias point of the FP section. The narrow beatnote feature is maintained throughout the *entire* dynamic range of lasing, implying that the bias-dependent dispersion can be well balanced by the electrically tunable DC section. Imperfections do exist. For example, from 0.87 to 0.97 A there are side peaks on both sides of the main beatnote that are 45 dB below the main peak, which implies that the dispersion is nearly breaking the coherence of the comb state. A more robust DC scheme or a compensator dealing with higher-order dispersion will be a

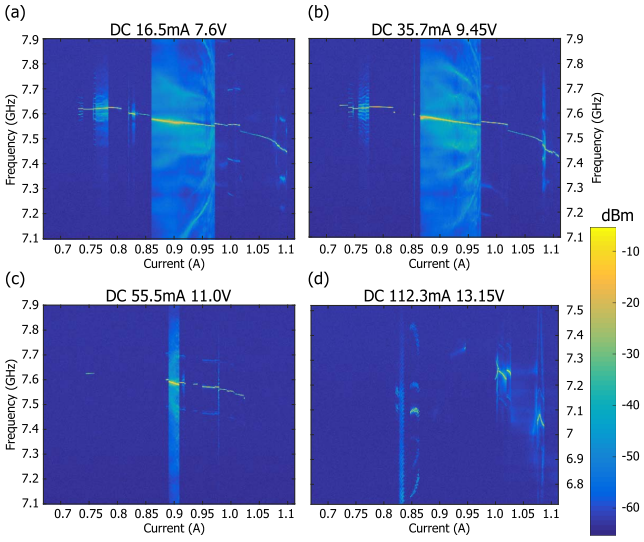

Fig. 3. Repetition-rate maps in the same biasing range (as in Fig. 2), while keeping the DC section at various static biasing points. (a) DC section is under 16.5 mA; (b) the DC section is under 35.7 mA; (c) the DC section is under 55.5 mA; (d) the DC section is under 112.3 mA.

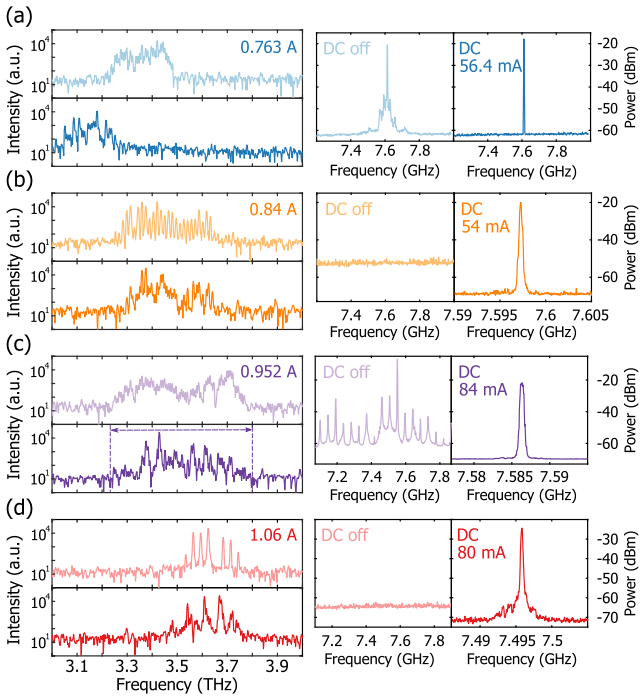

Fig. 4. (a)–(d) Terahertz spectra and repetition-rate spectra. Different colors imply different bias points of the FP section, while light and dark colors pair the terahertz spectrum with corresponding to a repetition-rate spectrum. The light color always represents the data when the DC section is unbiased, while the dark color shows the data in comb mode when the DC section is under optimized bias. The optimal DC biases for the data shown here are (a) 56.4 mA, (b) 54 mA, (c) 84 mA, and (d) 80 mA for.

method to further address this issue [13]. Since the DC section is optimized to cancel the FP section's dispersion at one designed biasing point, its tunability only needs to be enough to balance the portion of the dispersion that deviates from the designed biasing point. In order to achieve the full dynamic range comb performance, adjusting the bias of the DC section is fairly easy—one only needs to tune its bias when the beatnote starts deviating from a narrow beatnote.

To verify that dispersion management comes from the tunability of the DC, the device's repetition-rate beatnote maps are investigated at various static bias points of the DC section and shown in Fig. 3. Comparing Figs. 3(a) and 3(b), increasing the DC section's bias helps to stretch the comb regime between 0.77 and 0.82 A, as well as a comb regime above 1 A. Furthermore, as shown in Fig. 3(c), when the DC section is biased at 55.5 mA, the broad beatnote regime between 0.86 and 0.97 A starts transforming into a single beatnote regime. Improper tuning, on the other hand, does hurt the comb operation. For example, in Fig. 3(d), the bias on the DC section is too high, and no single beatnote regime is formed *anywhere* within the dynamic range.

The lasing spectra at several FP bias points are also investigated, and a comparison between non-comb and comb states at such bias points, distinguished by the corresponding repetition-rate spectra, is shown in Fig. 4. Different colors indicate different bias points [same color dots shown in Fig. 2(a)]; while within one subfigure, color contrast illustrates the pairwise relationship between the terahertz spectrum and the repetition-rate beatnote spectrum. In all subfigures, the light color pair represents the data at the FP bias point when the DC section is unbiased, while the dark color pair represents the same FP bias point with an optimized DC section bias. All comb state data shown here are taken under a free-running condition, and their linewidths are in kHz range, mainly reflecting the environmental feedbacks to the comb states. Figures 4(a) and 4(d) illustrate the transformation from multi-mode lasing to comb operation, while Fig. 4(c) shows the device transforming from a multi-beatnote state into the coherent comb state. In Fig. 4(a), the lasing shifts to lower frequencies when the DC section is biased, indicating the bias on DC section is tuning the laser's gain as well. One special case is shown in Fig. 4(b): the device can form a comb with multiple-repetition-rate spacing (in the case, $2f_{\mathrm{rep}}$) and, by tuning the DC section's bias, we can restore the mode spacing to f_{rep} (see Fig. 5 for more information). As elaborated in Ref. [6], the gain medium used here features a double-peak gain curve, and the difference between biases favors different parts of the total gain. As shown in Fig. 4, this is indeed the case, and the tunability in the DC section enables the formation of combs in various portions of the gain while preserving the gain bandwidth. The broadest comb state spectrum, shown in Fig. 4(c) with dashed lines, covers about a 600 GHz bandwidth centering at 3.5 THz, and within the entire bias range of lasing, comb operation between 3 and 3.9 THz with an average spectral coverage of 400 GHz is also achieved. Even larger comb bandwidth coverage can be expected from a better DC design, compensating for higher-order dispersions.

To summarize, we have shown that a two-section configuration featuring an electrically tunable DC is an effective way to address the bias-dependent dispersion. We have demonstrated a device exhibiting comb operation over its entire dynamic range of lasing, which will be helpful for frequency comb-based spectroscopy systems. In addition to compensating bias-dependent dispersion that destroys comb formation, this scheme

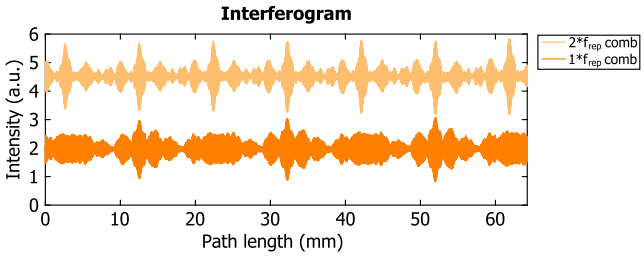

Fig. 5. Interferograms corresponding to the spectra in Fig. 4(b). The interferogram for the 2*frep comb is shown in light yellow, while the one for the 1*frep comb is shown in yellow.

may also be able to restore comb formation that is destroyed by external feedback, making comb operation more robust. The two-section configuration can also be implemented to QCL combs in other frequency regimes to solve similar issues, provided that fabrication challenges can be met. Furthermore, such a design can be naturally adapted to conduct active mode locking of QCLs [14–16], where the DC section can act as a modulator.

Funding. Defense Advanced Research Projects Agency (DARPA) (W31P4Q-16-1-0001); National Science Foundation (NSF).

Acknowledgment. This work in this Letter was performed, in part, at the Center for Integrated Nanotechnologies, an Office of Science User Facility operated for the U.S. Department of Energy (DOE) Office of Science. Sandia National Laboratories is a multimission laboratory managed and operated by National Technology and Engineering Solutions of Sandia, LLC., a wholly owned subsidiary of Honeywell International, Inc., for the U.S. Department of Energy's National Nuclear Security Administration under contract DE-NA-0003525.

REFERENCES

1. A. Hugi, G. Villares, S. Blaser, H. C. Liu, and J. Faist, Nature **492**, 229 (2012).
2. D. Burghoff, T.-Y. Kao, N. Han, C. W. I. Chan, X. Cai, Y. Yang, D. J. Hayton, J.-R. Gao, J. L. Reno, and Q. Hu, Nat. Photonics **8**, 462 (2014).
3. W. J. Wan, H. Li, T. Zhou, and J. C. Cao, Sci. Rep. **7**, 44109 (2017).
4. Y. Yang, D. Burghoff, D. J. Hayton, J.-R. Gao, J. L. Reno, and Q. Hu, Optica **3**, 499 (2016).
5. P. Friedli, H. Sigg, B. Hinkov, A. Hugi, S. Riedi, M. Beck, and J. Faist, Appl. Phys. Lett. **102**, 222104 (2013).
6. D. Burghoff, Y. Yang, J. L. Reno, and Q. Hu, Optica **3**, 1362 (2016).
7. M. Rosch, G. Scalari, M. Beck, and J. Faist, Nat. Photonics **9**, 42 (2015).
8. J. Faist, G. Villares, G. Scalari, M. Rosch, C. Bonzon, A. Hugi, and M. Beck, Nanophotonics **5**, 272 (2016).
9. C. Xu and D. Ban, Opt. Express **24**, 13500 (2016).
10. D. Burghoff, T.-Y. Kao, D. Ban, A. W. M. Lee, Q. Hu, and J. Reno, Appl. Phys. Lett. **98**, 061112 (2011).
11. M. Wienold, B. Röben, L. Schrottke, and H. T. Grahn, Opt. Express **22**, 30410 (2014).
12. D. Burghoff, Y. Yang, D. J. Hayton, J.-R. Gao, J. L. Reno, and Q. Hu, Opt. Express **23**, 1190 (2015).
13. Y. Yang, D. P. Burghoff, J. Reno, and Q. Hu, in *Conference on Lasers and Electro-Optics* (Optical Society of America, 2017), paper STh4O.4.
14. C. Y. Wang, L. Kuznetsova, V. M. Gkortsas, L. Diehl, F. X. Kärtner, M. A. Belkin, A. Belyanin, X. Li, D. Ham, H. Schneider, P. Grant, C. Y. Song, S. Haffouz, Z. R. Wasilewski, H. C. Liu, and F. Capasso, Opt. Express **17**, 12929 (2009).
15. S. Barbieri, M. Ravaro, P. Gellie, G. Santarelli, C. Manquest, C. Sirtori, S. P. Khanna, E. H. Linfield, and A. G. Davies, Nat. Photonics **5**, 306 (2011).
16. Y. Wang and A. Belyanin, Opt. Express **23**, 4173 (2015).